Cholangiocarcinoma in a cat infected with domestic cat hepatitis B virus

Haruka Dosaka,[1,#] Nanami X Kato,[2,#] Kei Taga,[3,#] Soshin Yamamoto,[3] Kaito Kondo,[1] Rissar Siringo Ringo,[2,5] Yasuyuki Kaneko,[4] Takuya Hirai,[1,5] Akatsuki Saito,[2,5,6,*] Naoyuki Fuke[1,*]

[1]Department of Veterinary Pathology, Faculty of Agriculture, University of Miyazaki, Miyazaki, Japan (DH, KK, HT, NF)

[2]Laboratory of Veterinary Microbiology, Department of Veterinary Science, Faculty of Agriculture, University of Miyazaki, Miyazaki, Japan (NXK, RSR, AS)

[3]Tokyo Cat Specialists, Minato-ku, Tokyo, Japan (KT, SY)

[4]Veterinary Teaching Hospital, Faculty of Agriculture, University of Miyazaki, Miyazaki, Japan (YK)

[5]Graduate School of Medicine and Veterinary Medicine, University of Miyazaki, Miyazaki, Japan (RSR, AS, TH)

[6]Center for Animal Disease Control, University of Miyazaki, Miyazaki, Japan (AS)

[#] These authors contributed equally.

* Corresponding authors:

Akatsuki Saito (sakatsuki@cc.miyazaki-u.ac.jp)

Laboratory of Veterinary Microbiology, Department of Veterinary Science, Faculty of Agriculture, University of Miyazaki, Miyazaki, 8892192, Japan

Tel: +81-985-58-7275; Fax: +81-985-58-7275

Naoyuki Fuke (fuke.naoyuki.z2@cc.miyazaki-u.ac.jp)

Department of Veterinary Pathology, Faculty of Agriculture, University of Miyazaki, Miyazaki, Miyazaki 8892192, Japan

26 Tel: +81-985-58-7271; Fax: +81-985-58-7271

Abstract

Cholangiocarcinoma is a rare hepatic malignancy in domestic cats, and its etiology remains largely undefined. Domestic cat hepadnavirus (DCHBV), a recently discovered member of the *Orthohepadnavirus* genus, shares similarities with human hepatitis B virus (HBV), which is associated with liver cancers, including cholangiocarcinoma. Here, we report a case of cholangiocarcinoma in a feline immunodeficiency virus-positive, 17-year-old spayed female cat infected with DCHBV. The patient presented with persistent vomiting, anorexia, and an elevated globulin level. Ultrasound revealed multiple hypoechoic hepatic lesions, and histopathology confirmed cholangiocarcinoma. Using quantitative PCR, DCHBV was detected in the spleen and ascitic fluid, and full-genome sequencing identified a unique 12-base deletion in both the polymerase and surface protein genes. Immunohistochemistry and RNA *in situ* hybridization demonstrated DCHBV core protein and mRNA expression in both tumor and non-tumor liver tissues, though signals were more prominent in non-neoplastic hepatocytes. The tumor exhibited CK7 positivity and HepPar-1 negativity, confirming biliary origin. While the causal relationship between DCHBV and cholangiocarcinoma remains to be clarified, the presence of a viral antigen and mRNA in neoplastic tissue suggests a potential role for DCHBV in hepatobiliary carcinogenesis. This is the first report describing cholangiocarcinoma in a cat with DCHBV infection, raising the possibility that DCHBV may have broader pathogenic potential beyond hepatitis and hepatocellular carcinoma.

Keywords

cat, cholangiocarcinoma, domestic cat hepadnavirus, immunohistochemistory, in situ hybridization

52 **Introduction**

53 Cholangiocarcinoma was the first type of bile duct malignancy reported in
54 dogs, [11, 30, 53, 73] cats,[10, 30, 52, 54] cattle, [3, 9, 14] horses, [6, 21] goats, [24] and wild animals. [46]
55 Cholangiocarcinoma cells express epithelial markers such as cytokeratin (CK) 7,
56 CK19, and claudin-7. [34] In dogs, the incident rate of cholangiocellular carcinoma is
57 estimated to be 0.36% of all tumors.[68] Hirose et al. reported that cholangiocellular
58 carcinoma in cats was 1 case (1.4%) of 71 feline liver biopsies at the Veterinary
59 Medical Center of the University of Tokyo.[30] Some studies have reported
60 cholangiocellular carcinomas as the most common primary hepatic malignancy in
61 cats, though this finding is inconsistent across all surveys.[10, 45, 52, 54, 76] The typical
62 age of cats diagnosed with cholangiocellular carcinomas is usually greater than 9
63 years.[42, 52] In two studies, female cats appeared at a higher risk for this neoplasm,
64 while another study found a higher incidence in male cats.[42, 52] There is no apparent
65 breed predisposition for cholangiocellular carcinoma in cats.[22] Like dogs, intrahepatic
66 cholangiocellular carcinomas are far more prevalent than those originating in the
67 extrahepatic bile ducts or gallbladder.[11, 45, 53, 76]

68 The pathogenesis of cholangiocarcinoma in animals is suspected to be
69 caused by factors such as parasites, chronic inflammation, genetic factors,
70 chemicals, and aging.[19, 20, 27, 29, 31, 48, 66] In humans, the hepatitis B (HBV) and
71 hepatitis C viruses can cause chronic hepatitis, increasing the risk of cirrhosis, liver
72 cancer (hepatocellular carcinoma), and cholangiocarcinoma.[43, 64] Persistent bile duct
73 inflammation in the liver, arising as chronic hepatitis and cirrhosis progress, may
74 induce mutations in bile duct cells, potentially leading to cholangiocarcinoma.[25] In
75 HBV infection, the virus directly affects liver and bile duct cells, promoting their
76 carcinogenesis.[74] Liver flukes (parasites in the *Opisthorchiidae* family) are strongly

associated with cholangiocarcinoma in South Asia.[16] They infect the bile ducts, causing chronic inflammation that can lead to cholangiocarcinoma if the infection continues for a long time.[63] Chemicals secreted by these parasites and the chronic inflammation caused by the infestation can stimulate the epithelial cells of the bile duct, promoting cancer.[63]

Viruses in the *Orthohepadnavirus* genus within the *Hepadnaviridae* family, including HBV, are known to cause liver diseases, such as hepatitis, cirrhosis, and hepatocellular carcinomas in humans, apes, woodchucks, and birds.[12, 15, 33, 40, 69] In 2018, a novel virus similar to HBV was identified in a domestic cat and is now referred to as domestic cat HBV (DCHBV). This marked the first reported case of hepadnavirus infection in a companion animal.[2] A recent study on canine serum samples revealed hepadnaviral DNA closely related to DCHBV.[23]

DCHBV is a small DNA virus measuring 42–50 nm in diameter. Its genome comprises circular, partially double-stranded DNA, approximately 3.2 kb long. Similar to other hepadnaviruses, the genome includes four overlapping open reading frames that code for polymerase (L), surface (S), core (C), and X proteins.[2, 47] DCHBV has been found in Brazil, Hong Kong, Italy, Japan, Malaysia, Taiwan, Thailand, Turkey, the United Kingdom, and the United States.[1, 2, 5, 17, 23, 35, 39, 56, 62, 67, 70, 72]

DCHBV shares clinical similarities with HBV and is often linked to immunosuppressive conditions in cats infected with feline immunodeficiency virus.[2, 5, 56, 70] The pathogenicity of DCHBV has been suggested to be associated with chronic hepatitis and hepatocellular carcinoma; however, it remains poorly understood. In the present study, we successfully detected DCHBV in a cat diagnosed with cholangiocarcinoma. Although further investigation is needed to determine whether

101 DCHBV is a causative factor of cholangiocarcinoma, our findings raise the possibility

102 that DCHBV may be associated with a previously unrecognized pathogenicity.

Materials and Method

Case Information

A 17-year-old spayed domestic shorthair cat, positive for feline immunodeficiency virus, was presented with the chief complaint of frequent vomiting and loss of appetite (Day 0). The patient had a known medical history of stage 3 chronic kidney disease.

Clinical testing

The patient underwent a blood test and an abdominal ultrasound. Blood tests included complete blood count and blood chemistry. The test items for blood chemistry were as follows: glucose, creatinine, blood urea nitrogen, phosphate, calcium, sodium, potassium, chloride, total protein, albumin, globulin, alanine aminotransferase, alkaline phosphatase, γ-glutamyltransferase, bilirubin, and cholesterol. The complete blood count was measured using IDEXX Procyte Dx (IDEXX Laboratories, Tokyo, Japan), and blood chemistry was run by IDEXX Catalyst One (IDEXX). The abdominal ultrasound was performed using LOGIQ10 (GE Healthcare, Tokyo, Japan). The patient was treated with prednisolone, cefovecin, and maropitant.

Detection of domestic cat HBV (DCHBV)

DNA samples were extracted from the cat's ascites, liver, and spleen using a DNeasy Blood & Tissue Kit (250) (Qiagen, Tokyo, Japan, Cat# 69506). We used a duplex real-time PCR assay to detect DCHBV from these DNA samples using Probe qPCR Mix (TaKaRa, Kusatsu, Japan, Cat# RR391B).[61] The primers/probe for DCHBV were forward primer (5'-ACTCACCAACTTCCTGTCCT-3'), reverse primer

128 (5’-CTTCCAATCCAGGAGAACCAAC-3’), and probe (/56-
129 FAM/ATCATTTAC/Zen/CTCTTGCTCCTGGCG/3IABkFQ/) (Integrated DNA
130 Technologies, Coralville, IA, USA). The primers/probe for the cat *Actb* gene were
131 forward primer (5’-TCTCGATCTGTGCAGGGTATTA-3’), reverse primer (5’-
132 AGACCGGCAAGACAGAAATG-3’), and probe
133 (/5HEX/TGGCAAGAG/ZEN/TCCTGAACCAGTTGT/3IABkFQ/) (Integrated DNA
134 Technologies). The analysis was performed using the QuantStudio 5 Real-Time PCR
135 System (Applied Biosystems, Waltham, MA, USA). The PCR conditions were 95℃ for
136 20 sec, followed by 40 cycles of 95℃ for 3 sec and 60℃ for 30 sec.
137
138 *Sequencing of the DCHBV genome*
139 We amplified the DCHBV genome collected from the spleen using
140 PrimeSTAR® Max DNA Polymerase Ver. 2 (TaKaRa, Cat# R047B). The primers were
141 DCHBV-1F (5’-ACTCTCAAACAGGG-AACATTCGTA-3’) and DCHBV-4R (5’-
142 GTCTAGATTGT-GACGAGGGAAAAAC-3’), for amplifying Fragment 1F-4R, and
143 DCHBV-4F (5’-GAAGAGGAACTT-ACAGGTAGGGAAC-3’) and DCHBV-6R (5’-
144 CATCCATATAAGCAAACACCATACA-3’), for amplifying Fragment 4F-6R. The PCR
145 conditions were 40 cycles at 98°C for 10 sec, 55°C for 5 sec, and 68°C for 30 sec,
146 followed by 68°C for 7 min. The amplicons were visualized in a 0.6% agarose gel.
147 Each amplicon was extracted from the gel using the QIAquick Gel Extraction Kit
148 (Qiagen, Cat# 28706). We then sequenced the entire viral genome using eight pairs
149 of primers, as shown in **Supplementary Table S1**. The sequences of the amplicons
150 were determined using a SupreDye v3.1 Cycle Sequencing Kit (M&S
151 TechnoSystems, Osaka, Japan, Cat# 063001) with the Spectrum Compact CE
152 System (Promega, Madison, WI, USA). We used a Gel Filtration Cartridge (M&S

TechnoSystems, Cat# 42453) to purify the amplicons used for sequencing. The sequence assembly was performed using 4Peaks (Nucleobytes, Aalsmeer, The Netherlands) and Microsoft Word 2019 (Microsoft, Redmond, WA, USA). The sequence of the strain identified in this study was aligned with domestic cat hepadnavirus Japan/KT116/2021 using MEGA X (MEGA Software) (Version 11.0.13).

Phylogenic analysis of viral proteins

A phylogenetic tree was constructed using the *Hepadnaviridae* protein (polymerase, core protein, X protein, surface protein) sequences obtained from GenBank for *Hepadnaviridae* protein. The tree was created using the MUSCLE algorithm in MEGA X. We subsequently constructed a phylogenetic tree from the aligned amino acid sequences from public databases. Evolutionary analyses were performed using the maximum likelihood and neighbor-joining methods, employing the Jones–Taylor–Thornton matrix-based model.

Sequence alignment and pairwise identity calculation for nucleotide and protein sequences

Pairwise nucleotide and amino acid sequence identities were calculated using MEGA X. Sequences were aligned with MUSCLE implemented in MEGA, and pairwise distances were computed using the *p-distance* model, with complete deletion of gaps. Because MEGA provides *p-distance* as the proportion of nucleotide differences between each pair of sequences, the percentage identity was subsequently calculated as (1 − p-distance) × 100. The alignment was manually checked and edited to minimize artificial gaps and ensure accurate comparisons.

178 *Polyclonal antibody production*

179 Polyclonal antibodies were generated by Eurofins Genomics (Tokyo, Japan)
180 using their standard rabbit immunization protocol. The antigens, synthetic peptides
181 corresponding to DCHBV core protein (NH2-C+DLVDTIQALYEEELTGREH-COOH),
182 were designed and synthesized by Eurofins. These amino acid sequences are
183 conserved between the reference strain of DCHBV, the DCHBV (Sydney) strain
184 (Accession number: MH307930.1),[2] and a Japanese strain DCHBV (KT116)
185 (Accession number: LC668427.1) we identified.[70] The peptide was conjugated to
186 keyhole limpet hemocyanin to enhance immunogenicity. Two New Zealand White
187 rabbits were immunized over a 49-day protocol involving four antigen injections.
188 Serum samples were collected pre- and post-immunization. Affinity purification was
189 performed using a peptide-conjugated column to obtain antigen-specific antibodies.
190

191 *Plasmids*

192 To generate plasmids encoding HA-tagged *Orthohepadnavirus* core proteins,
193 HBV (genotype A) (Accession number: LC488828.1), DCHBV (KT116), or
194 Woodchuck hepatitis virus (WHV) (Accession number: NC_004107.1)-derived
195 sequences codon-optimized to human cells were synthesized by Twist Bioscience
196 (South San Francisco, CA, USA). The synthesized DNA sequence is summarized in
197 **Supplementary Table S2**. The synthesized DNA was cloned into a pCAGGS
198 plasmid,[49] which was pre-linearized with EcoRI–HF (New England Biolabs, Ipswich,
199 MA, USA, Cat# R3101M) and NheI–HF (New England Biolabs, Cat# R3131L) using
200 an In-Fusion HD Cloning Kit (TaKaRa, Cat# Z9633N). The plasmids were amplified
201 using NEB 5-alpha F' *Iq* competent *Escherichia coli* (New England Biolabs, Cat#

202 C2992H) and extracted using the PureYield Plasmid Miniprep System (Promega,
203 Cat# A1222). The sequences of all plasmids were verified as described above.
204
205 *Cell Culture*
206 Lenti-X 293T cells (TaKaRa, Cat# Z2180N) were cultured in Dulbecco's
207 modified Eagle's medium (Nacalai Tesque, Kyoto, Japan, Cat# 08458-16)
208 supplemented with 10% fetal bovine serum (Cytiva, Marlborough, MA, USA, Cat#
209 SH30396) and 1× penicillin–streptomycin (Nacalai Tesque, Cat# 09367-34) at 37°C
210 in a humidified incubator with 5% CO_2.
211
212 *Western blotting*
213 To obtain cellular lysates containing *Orthohepadnavirus* core protein, Lenti-X
214 293T cells were seeded into a 12-well plate (FUJIFILM Wako Pure Chemical, Osaka,
215 Japan, Cat# 636-28421) at 2.5×10^5 cells/well, cultured overnight, and transfected
216 with one µg of pCAGGS–HA–HBV (A)–Core plasmid, pCAGGS–HA–DCHBV
217 (KT116)–Core plasmid, pCAGGS–HA–WHV–Core plasmid or pCAGGS empty
218 plasmid using TransIT-LT1 Ttransfection Reagent (TaKaRa, Cat# V2304T) in Opti-
219 MEM (Thermo Fisher Scientific, Waltham, MA, USA, Cat# 31985062). After 48 hours
220 of incubation, the cellular pellets were collected and lysed with 2× Bolt LDS sample
221 buffer (Thermo Fisher Scientific, Cat# B0008) containing 2% β-mercaptoethanol (Bio-
222 Rad, Hercules, CA, USA, Cat# 1610710) and incubated at 70°C for 10 min. The
223 expression levels of core protein were assessed using SimpleWestern Abby
224 (ProteinSimple, San Jose, CA, USA) with rabbit anti–core polyclonal antibodies
225 (Eurofins Genomics, 1:20 dilution) and an anti–rabbit detection module
226 (ProteinSimple, Cat# DM-001A). The expression of HA-tagged proteins was

227 analyzed with an anti–HA Tag (6E2) mouse monoclonal antibody (CST, Danvers, MA,
228 USA, Cat# 2367S, x200) and an anti–mouse detection module (ProteinSimple, Cat#
229 DM-002). The amount of input protein was measured using the total protein detection
230 module (ProteinSimple, Cat# DM-TP01). The predicted sizes of the DCHBV (KT116)
231 core protein were calculated according to the Protein Molecular Weight website
232 (https://www.bioinformatics.org/sms/prot_mw.html, accessed on November 13,
233 2024).
234
235 *Histopathological examination*
236 Tissue samples were fixed in 10% formalin and embedded in accordance with
237 standard procedures, sectioned at 3μm, and stained with hematoxylin and eosin
238 (HE).
239
240 *Immunohistochemical examination*
241 Immunohistochemical staining (IHC) was performed using the following
242 primary antibodies: Hepatocyte (HerPar-1, clone: OCH1E5, Dako, Tokyo, Japan,
243 Cat# M7158,) (1:25), cytokeratin 7 (CK7) (clone: OV-TL12/30, Dako, Cat# M7018)
244 (1:50), and DCHBV Core (57-75) (1: 2,000). The secondary antibody used was
245 Histofine Simple Stain MAX-PO (MULTI) (Nichirei Biosciences, Tokyo, Japan, Cat#
246 424144). For IHC, after deparaffinization and rehydration, antigen retrieval was
247 performed as follows: HapPar-1 and DCHBV core were subjected to heat treatment
248 at 105℃ for 10 minutes using an antigen retrieval solution at pH 9.0, while CK7 was
249 activated with proteinase K (20 mg/mL, TaKaRa, Cat# 162-22751) (1:50) at 37℃ for 5
250 minutes. Endogenous peroxidase activity was blocked using 3% hydrogen peroxide
251 in methanol, followed by blocking with Blocking One (Nacalai Tesque, Cat# 03953-

95). The reaction conditions were 60 minutes at 37℃ for the primary antibody and 30 minutes at 37℃ for the secondary antibody. The chromogen was 0.05% 3, 3′-diaminobenzidine (Sigma-Aldrich, St. Louis, USA, Cat# SHBF5184V) and 0.03% hydrogen peroxide in a Tris-hydrochloric acid buffer (pH 7.6). Afterward, the sections were counterstained with hematoxylin for 15 seconds, rinsed, dehydrated in a graded series of ethanol, cleared with three changes of xylene, and mounted using a mounting solution. We used three cases as negative controls: feline hepatocellular carcinoma, cholangiocarcinoma, and normal liver.

RNA in situ hybridization

RNA *in situ* hybridization (RNA ISH) is commercially available as RNAscope (Advanced Cell Diagnostics, Hayward, CA, USA, Cat# 322300). This technique allows for the localization of gene expression within formalin-fixed, paraffin-embedded tissues. To assess the expression of DCHBV mRNA, RNA ISH (Advanced Cell Diagnostics) was performed according to the manufacturer's guidelines. Tissue sections were initially deparaffinized, then incubated with pretreat 1 reagent (Hydrogen Peroxide) at room temperature for 10 minutes. Subsequently, sections were treated with pretreat 2 reagent (Target Retrieval Buffer) at 105°C for 10 minutes and then incubated with pretreat 3 reagent (Protease Plus) at 40°C for 15 minutes. Sections were hybridized at 40°C for 2 hours with the hepadnavirus probe (Advanced Cell Diagnostics, Cat# 575811), the positive control probe Fc-PPIB (Advanced Cell Diagnostics, Cat# 455011), and the negative control probe DapB (Advanced Cell Diagnostics, Cat# 310043). Following hybridization, the signals were amplified and visualized using the RNA ISH 2.5 HD Detection Kit—BROWN (Advanced Cell

276 Diagnostics, Cat# 322310). Positive staining was identified by the presence of brown

277 punctate dots within the cytoplasm or nucleus.

Results

Clinical Course

On physical examination, the cat was underweight and dehydrated; however, no other significant abnormalities were noted. Hematological and biochemical analyses revealed an elevated serum globulin concentration (5.8 g/dL) and increased feline pancreatic lipase level (32 μg/L) (**Supplemental Table S3**). Abdominal ultrasonography revealed multiple hypoechoic, spot-like lesions distributed throughout the hepatic parenchyma, with no predilection for a specific liver lobe. The margins of the lesions were indistinct, and the liver surface appeared irregular to nodular with blunted edges (**Fig. 1a**). Fine needle aspiration was performed on the hepatic lesions, and cytological analyses revealed hepatocellular edema and glycogen-like degeneration. Initial treatment consisted of subcutaneous fluid therapy and oral prednisolone at a dosage of 1 mg/kg once daily. The patient's clinical condition showed mild improvement following treatment. The cat was re-evaluated on Day 81, due to recurrent inappetence and progressive weight loss. Repeat abdominal ultrasonography demonstrated hepatomegaly, in addition to the previously observed findings. Cefovecin (8 mg/kg, subcutaneously) was administered in combination with continued prednisolone therapy. On Day 95, the patient's general condition had significantly worsened, and euthanasia was elected. A complete necropsy was performed postmortem. Gross pathological findings included a markedly enlarged, firm liver with a coarse surface (**Fig. 1b**). A 15-mm milky-white mass was diffusely distributed throughout the hepatic tissue. Severe adhesions were observed between the liver, spleen, and diaphragm. Approximately 40 mL of ascitic fluid and 10 mL of pleural effusion were collected. No evidence of icterus was noted.

303 *Identification of DCHBV from Spleen and Ascitic Fluid Samples*

304 To assess the presence of DCHBV, we performed qPCR analyses on DNA
305 extracted from formalin-fixed liver tissue, frozen ascitic fluid, and frozen spleen
306 samples. Amplification of the feline *Actb* gene was used as an internal control to
307 verify sample quality and PCR efficiency.

308 Efficient amplification of the *Actb* gene was confirmed in the spleen and ascitic
309 fluid samples, indicating sufficient DNA quality for viral detection. Quantitative PCR
310 revealed that both the spleen and ascitic fluid samples were positive for DCHBV. In
311 contrast, the *Actb* gene was not amplified in the liver samples, rendering it impossible
312 to determine whether DCHBV was present or absent in these specimens, due to
313 insufficient or degraded DNA quality.

314

315 *Genetic Characteristics of the Identified DCHBV*

316 PCR amplicons covering the complete genome of DCHBV were successfully
317 obtained (**Fig. 2**), and the complete genome sequence of the isolate
318 Japan/MGR73/2024 was determined (deposited as LC856674.1). We constructed
319 phylogenetic trees based on each DCHBV protein (polymerase, surface, core, and X)
320 as well as the full-length nucleotide sequences (**Figs. 3a-e**).

321 The polymerase protein of Japan/MGR73/2024 showed the highest identity
322 (98.92%) with the HK12/2020/160775 strain (OP643862.1) (**Supplemental Table**
323 **S4**). It also shared 98.56% identity with the Japan/KT116/2021 strain (LC668427.1),
324 98.80% with the Japan/230206-13/2023 strain (LC830691.1), 98.20% with the
325 Sydney2016 strain (MH307930.1), and 86.43% with the Rara strain (LC685967.1,
326 Japan) (**Supplemental Table S4**). The surface protein of Japan/MGR73/2024 also
327 showed the highest identity (99.20%) with the Sydney2016 strain, CV-3/THA/2023

328 (PV392816.1), CV-5/THA/2023 (PV392817.1), SH-48/THA/2023 (PV392818.1),
329 DCH/NPUST-006/TWN/2023 (OR515504.1), catITA/2021/2 serum (OQ859619.1),
330 catITA/2021/2 effusion (OQ859620.1), and catITA/2021/1 serum (OQ859621.1)
331 (**Supplemental Table S5**). It displayed 98.94% with the Japan/KT116/2021 strain,
332 98.94% with the Japan/230206-13/2023 strain, and 92.31% with the Rara strain
333 (**Supplemental Table S5**). The core protein of Japan/MGR73/2024 exhibited the
334 highest similarity (100%) to the Japanese 53768 strain (LC756472.1) (**Supplemental**
335 **Table S6**). It also showed 99.54% identity with Japan/230206-13/2023 and
336 Sydney2016, 99.08% with Japan/KT116/2021, and 98.62% with the Rara strain
337 (**Supplemental Table S6**). The X protein was closely related to the
338 Japan/KT116/2021 strain, with 99.31% identity (**Supplemental Table S7**). Identity
339 levels with other strains were 98.62% for the Japan/230206-13/2023 strain, 96.55%
340 for the Sydney2016 strain, and 79.31% for the Rara strain (**Supplemental Table S7**).
341 The full genome sequence of Japan/MGR73/2024 showed the highest identity
342 (99.21%) with the Japan/230206-13/2023 strain (**Supplemental Table S8**). It also
343 shared 99.09% identity with the Japan/KT116/2021 strain, 98.08% with the
344 Sydney2016 strain, and 79.31% with the Rara strain (**Supplemental Table S8**).
345 Interestingly, a 12-base deletion (nucleotide positions 2954–2965, based on
346 the Japan/KT116/2021 strain) was identified in the MGR73/2024 strain (**Fig. 3e**). This
347 deletion resulted in the loss of four amino acids in the polymerase (positions 267–
348 270) and surface (positions 79–82) proteins. In the surface protein, the deleted
349 residues were located within the Pre-S1 region of the large surface protein. We also
350 found that this deletion was confirmed in JAPAN/MGR73/2024, which was extracted
351 from the liver (**Fig. 3f**).
352

353 *Pathological analyses of liver*

354 To validate the specificity of the rabbit polyclonal antibody targeting the
355 DCHBV core protein, we first assessed its reactivity by evaluating core protein
356 expression in mammalian cells. HA-tagged expression plasmids encoding the core
357 proteins of DCHBV, HBV, and WHV were constructed and transfected into
358 mammalian cells. Western blot analysis using an anti-HA monoclonal antibody
359 confirmed efficient expression of the HA-tagged core proteins (**Fig. 4a**).
360 Subsequently, the reactivity of the rabbit anti-DCHBV core polyclonal antibody was
361 examined. The antibody specifically recognized the DCHBV core protein, but did not
362 cross-react with the core proteins of HBV or WHV (**Fig. 4b**). These results indicate
363 that the polyclonal antibody generated in this study exhibits high specificity for the
364 DCHBV core antigen and is suitable for detecting DCHBV in liver tissue samples.

365 The mass was multinodular, white to grayish-white, and 4×3×1.5 cm in
366 diameter (**Fig. 5a**). After formalin fixation, the cut surface was a solid pale yellow to
367 white lesion (**Fig. 5b**). The boundary between the tumor and normal tissue was clear.
368 In histopathological examinations, neoplastic tissue infiltrated and proliferated within
369 the liver parenchyma without a capsule (**Fig. 5c**). The neoplastic cells were arranged
370 in a tubular structure and contained an eosinophilic substance (**Fig. 5d**). The
371 neoplastic cells were cuboidal to columnar form, similar to bile epithelial cells. The
372 nuclei were round to oval, exhibiting anisokaryosis and containing one to several
373 prominent nuclei. A mitotic count of 35 per 10 high-power fields was observed. Some
374 neoplastic cells were found in the blood or lymphatic vessels. Connecting tissue
375 proliferated between neoplastic areas. In non-neoplastic tissue, diffuse hepatocellular
376 vacuolar degeneration and loss of nuclei were observed with hepatocytes containing

377 brown pigments (**Fig. 5e**). Mild inflammation was present in the portal area, and a
378 few neutrophils were observed in the sinusoids (**Fig. 5f**).
379
380 *Immunohistochemical analyses of liver*
381 CK7 was positive in the cytoplasm of neoplastic cells and bile duct epithelial
382 cells, and negative in hepatocytes (**Figs. 6a-c**). HepPar-1 was positive in the
383 cytoplasm of hepatocytes and negative in the neoplastic cells and bile duct epithelial
384 cells (**Figs. 6d-f**). DCHBV core was partially positive in the cytoplasm of neoplastic
385 cells, in bile duct epithelial cells and diffusely positive in the cytoplasm of
386 hepatocytes. (**Figs. 6g-i**).
387
388 *RNA in situ hybridization*
389 RNA ISH was performed to evaluate DCHBV mRNA expression status. A focal
390 positive signal was detected in the nuclear and cytoplasm of degenerated or normal
391 hepatocytes and neoplastic cells (**Figs. 7a-b**). A total of 133 signals were observed in
392 10 high-power fields within the neoplastic cells area, whereas 526 signals were
393 identified in the non-neoplasmic area. These findings indicate that the number of
394 signals in the tumor area was lower than in the non-tumor area. The positive signal in
395 the cytoplasm of hepatocytes was diffusely distributed in a fine granular pattern.

396 **Discussion**

397 In this study, we report a case of cholangiocarcinoma in a cat infected with
398 DCHBV. Full-genome sequencing suggested that the DCHBV strain identified in this
399 study is genetically close to Japanese strains. Furthermore, we identified a unique
400 12-base deletion in both the polymerase and surface protein genes, suggesting a
401 distinctive evolution of DCHBV in the cat. Our pathological investigation revealed the
402 presence of DCHBV core protein and mRNA expression in both tumor and non-tumor
403 liver tissues. Notably, the tumor exhibited CK7 positivity and HepPar-1 negativity,
404 suggesting a biliary origin. This is the first report describing cholangiocarcinoma in a
405 cat with DCHBV infection, raising the possibility that DCHBV may have broader
406 pathogenic potential beyond chronic hepatitis and hepatocellular carcinoma.

407 We detected DCHBV from a cat that died with symptoms associated with
408 cholangiocarcinoma and determined the complete viral genome sequence. Based on
409 the results shown in **Supplemental Table S8**, JAPAN/MGR73/2024 showed high
410 homologies with those identified in Japan; however, we also found that
411 JAPAN/MGR73/2024 did not match flawlessly with any DCHBV strains identified in
412 Japan. Therefore, we concluded that JAPAN/MGR73/2024 has evolved
413 independently in Japan.

414 We found a 12-base deletion (compared with the Japan/KT116/2021 strain) or
415 a 15-base deletion (compared with the Sydney2016 strain) in JAPAN/MGR73/2024.
416 To our knowledge, this is the largest deletion in the DCHBV genome. Although it is
417 difficult to conclude that JAPAN/MGR73/2024 is solely responsible for the
418 cholangiocarcinoma in cats, DCHBV likely contributes to the development of
419 cholangiocarcinoma.

420 A recent study showed that the spacer domain, which spans amino acid
421 residues 184–348 in HBV, is an intrinsically disordered protein and a poorly
422 conserved region in HBV polymerase.[44] HBV tolerates deletions and insertions
423 without significant influence on polymerase functions.[57] In addition, it has been
424 revealed that polymerase activity remains intact even with a large deletion within the
425 spacer domain, and only amino acid residues 293–335 are required to retain enzymic
426 activity.[58] By contrast, functional changes, such as incapability or a decrease of RNA
427 packaging efficiency, reduced polymerase activity, and increased stability of the P
428 protein, have been related to the deletion of amino acids in the spacer domain.[7, 8, 32,
429 36, 37, 38, 58] Therefore, clarifying the functional changes in the polymerase imposed by
430 the deletion of amino acid residues 267–270 in DCHBV JAPAN/MGR73/2024 is
431 essential.
432 Previous papers have also shown that four of the ten amino acid residues
433 used to distinguish the HBV genotype were in the surface protein.[44] However, to the
434 best of our knowledge, it remains unclear whether this difference in genotype can
435 impact the function of a surface protein or not. In addition, a recent study reported
436 that the epitope of HBV is located in amino acid residues 33–47, and an amino acid
437 substitution at the 45th residue significantly reduced the antigenicity of HBV.[26]
438 Therefore, it is critical to test whether the deletion of amino acid residues 267–270
439 found in DCHBV JAPAN/MGR73/2024 affects functions, including antigenicity and
440 entry into the target cells.
441 Cholangiocarcinoma is a malignant tumor originating from the intrahepatic biliary
442 epithelium. Microscopically, it appears as a well-differentiated type consisting of
443 glandular or acinar proliferative foci of bile duct epithelial cells. In contrast, poorly
444 differentiated types exhibit acinar proliferative areas within solid proliferative foci.

445 Moreover, the undifferentiated type exhibits an island- or cord-like growth pattern with
446 squamous metaplasia.[22, 28] In cats, it is usually covered by a fibrous capsule and
447 characterized by increased fibrous components within the tumor. [10, 30, 52] In the
448 present case, glandular proliferation and increased connective fibers were noted.
449 Additionally, the infiltrative growth into blood vessels and surrounding tissues further
450 supports the diagnosis of a malignant tumor originating from the biliary epithelium.
451 Differential diagnoses include hepatocellular carcinoma, metastatic epithelial
452 malignancies, and hepatic carcinoid. Hepatocellular carcinoma is classified into
453 trabecular, pseudoglandular, and solid types, with tumor cells demonstrating a
454 cuboidal to columnar morphology, minimal stromal fibrosis, and no mucus
455 production.[22, 28] Cholangiocarcinoma is CK7-positive and HapPar-1-negative,
456 whereas hepatocellular carcinoma is CK7-negative and HapPar-1-positive.[34, 59] In the
457 case presented, CK7-positive neoplastic cells proliferated while forming lumens
458 containing mucus and were accompanied by fibrosis, supporting a
459 cholangiocarcinoma diagnosis. Metastatic tumors may arise in cats from malignant
460 epithelial tissues, including those of the gallbladder or pancreas.[13, 22, 28, 51] While
461 immunohistochemical markers such as CK7 can aid in differentiation, distinguishing
462 these tumors is generally challenging in HE.[22, 28] In the present case, no tumor
463 lesions were identified in other organs, suggesting a low likelihood of metastases.
464 Hepatic carcinoid is a tumor derived from neuroendocrine cells and exhibits growth
465 patterns such as rosette, ribbon, and solid formations. It is distinguished by positive
466 immunostaining for neuron-specific enolase.[22, 28]
467 While primary hepatobiliary tumors in cats are rare, previous studies have
468 been reported.[10, 18, 52] Factors associated with cholangiocellular carcinoma
469 development include infection with liver flukes or intestinal parasites,[4, 65] exposure to

470 chemical substances such as plutonium and americium,[71] and chronic
471 inflammation.[60] Certain animal viruses are known to contribute to tumor development.
472 Hepadnaviruses exhibit strong hepatotropism and host specificity and are
473 responsible for acute and chronic hepatitis, liver cirrhosis, and hepatocellular
474 carcinoma.[22] In humans, HBV has been suggested to increase the risk of
475 cholangiocarcinoma.[43, 64] Potential mechanisms by which hepadnaviruses promote
476 cholangiocarcinoma include carcinogenesis driven by chronic inflammation,[43] the
477 inactivation of tumor suppressor genes by HBx, a gene product of hepadnavirus,[75]
478 abnormal differentiation or transformation of cholangiocytes,[64] and integration of the
479 hepadnaviral DNA genome[50]. A similar association with cholangiocarcinoma is
480 plausible, since human HBV is closely related to DCHBV.[2, 5, 39, 56] Previous reports
481 have suggested a link between DCHBV and chronic hepatitis or hepatocellular
482 carcinoma.[55] While the oncogenic mechanisms and relationship between the
483 detected DCHBV and cholangiocarcinoma remain unclear, viral antigens in the tumor
484 and liver cells suggest that viral infection may play a role in carcinogenesis.
485 In our investigation, DCHBV mRNA was detected in hepatocytes rather than
486 neoplastic cells, and hepatocellular degeneration and inflammation were also
487 present. Considering those findings, DCHBV may infect liver cells, leading to
488 degeneration and inflammation, which may subsequently trigger the development of
489 cholangiocarcinoma.
490 In conclusion, while additional studies are required to clarify whether DCHBV
491 directly contributes to the development of cholangiocarcinoma, our findings suggest
492 that DCHBV may be linked to a previously unidentified aspect of pathogenicity.

Acknowledgments

The authors thank Ms. Miki Kawano, Ms. Natsumi Matsubara, Ms. Tomoko Nishiuchi, Dr. Maya Shofa, and the staff of CADIC, University of Miyazaki, for their assistance.

Funding

This work was supported by grants from the Japan Agency for Medical Research and Development (AMED) Research Program on HIV/AIDS JP25fk0410075h0001, JP24fk0410047, JP25fk0410056, and JP25fk0410058 (to A.S.); the AMED Research Program on Emerging and Re-emerging Infectious Diseases JP23fk0108583, and JP24fk0108907h0001 (to A.S.); the AMED the Research Project for Practical Applications of Regenerative Medicine JP24bk0104177 (to A.S.); the JSPS KAKENHI Grant-in-Aid for Scientific Research (C) JP24K09227 (to A.S.); the JSPS KAKENHI Grant-in-Aid for Scientific Research (B) JP22H02500 (to A.S.) and JP21H02361 (to A.S.); the JSPS Bilateral Program JPJSBP120245706 (to A.S.); the JSPS Fund for the Promotion of Joint International Research (International Leading Research) JP23K20041 (to A.S.); the G-7 Grants (2024) (to A.S.); Shionogi infectious disease research promotion foundation (2024) (to A.S.); and the Ito Foundation Research Grant R6 KEN119 (to A.S.) and R6 KEN161 (to N.F.).

Conflicts of Interest

The authors declare no conflict of interest.

514 **Figure legends**

515 **Figure 1.** Clinical findings in the patient cat. (**a**) The abdominal ultrasound reveals
516 multiple, rounded, hypoechoic lesions with poorly defined margins (arrowheads)
517 distributed diffusely throughout the hepatic parenchyma. The hepatic surface appears
518 irregular to nodular, with blunted edges. (**b**) Gross findings at necropsy. The liver
519 exhibits extensive adhesions to the peritoneum, stomach, spleen, and diaphragm.

520

521 **Figure 2.** Electrophoresis image of PCR amplicons. The DCHBV genomes collected
522 from the ascites and spleen were amplified by PCR.

523

524 **Figure 3.** Phylogenetic tree of DCHBV structural proteins. Phylogenetic trees of
525 DCHBV (**a**) polymerase protein, (**b**) surface protein, (**c**) core protein, and (**d**) X
526 protein were created using the MUSCLE algorithm in MEGA X software. Evolutionary
527 analyses were performed using the maximum likelihood and neighbor-joining
528 methods, employing the Jones–Taylor–Thornton matrix-based model. In the
529 phylogenetic trees, the red dot indicates the DCHBV strain identified in this study,
530 Japan/MGR73/2024. (**e**) Sequencing of DCHBV. The complete genome sequence of
531 JAPAN/MGR73/2024 was determined. The region where 12nt deletions were
532 observed in JAPAN/MGR73/2024 is indicated and was compared with other cases of
533 DCHBV (Sydney2016 and JAPAN/KT116/2021).

534

535 **Figure 4.** Western blot of DCHBV core protein. The expression levels of core protein
536 were assessed with (**a**) an anti–HA Tag (6E2) mouse monoclonal antibody or (**b**) an
537 anti–core rabbit polyclonal antibody.

538

539 **Figure 5.** Cholangiocarcinoma, liver, cat. **Figures 5a-b.** Gross appearance and cut
540 surface of the hepatic mass. (**a**) Multiple yellowish-white masses of varying sizes are
541 present on the liver surface. (**b**) Cut surface of the mass after formalin fixation. A solid
542 whitish tumor area is observable. **Figures 5c-d.** Histological findings of the tumor
543 region. (**c**) A capsule is formed between the normal and tumor tissues, with a clearly
544 demarcated boundary. Proliferation of connective tissue is observed in the stroma.
545 Hematoxyline and eosin (HE). (**d**) Neoplastic cells form luminal structures containing
546 eosinophilic serous fluid. The tumor cells are round to cuboidal in shape, and mitotic
547 figures are observed. HE. **Figures 5e-f.** Histological findings of hepatocytes outside
548 the neoplasm. (**e**) Hepatocytes show diffuse vacuolar degeneration, and nuclei are
549 absent in some cells. Neutrophils are observed in the sinusoids. HE. (**f**)
550 Predominantly lymphocytes are observed in the portal area. HE.
551
552 **Figure 6.** Cholangiocarcinoma, liver, cat. Immunohistochemical (IHC) results for
553 neoplastic cells, hepatocytes, and biliary epithelial cells. (**a**) Cytokeratin 7 (CK7) for
554 neoplastic cells. The cytoplasm of the tumor cells shows diffuse positivity for CK7.
555 IHC. (**b**) CK7 for hepatocytes. Hepatocytes are negative for CK7. IHC. (**c**) CK7 for
556 biliary epithelial cells. The cytoplasm of the biliary epithelial cells shows diffuse
557 positivity for CK7. IHC. (**d**) HepPar-1 for neoplastic cells. Tumor cells are negative for
558 HepPar-1. IHC. (**e**) HepPar-1 for hepatocytes. The cytoplasm of hepatocytes shows
559 diffuse positivity for HepPar-1. IHC. (**f**) HepPar-1 for biliary epithelial cells. Biliary
560 epithelial cells are negative for HepPar-1. IHC. (**g**) DCHBV core for neoplastic cells.
561 Tumor cells show partial positivity for DCHBV core. IHC. (**h**) DCHBV core for
562 hepatocytes. Hepatocytes show focal diffuse positivity for DCHBV core. IHC. (**i**)

563 DCHBV core for biliary epithelial cells. Biliary epithelial cells are negative for DCHBV
564 core. IHC.
565
566 **Figure 7.** Cholangiocarcinoma, liver, cat. **Figures 7a-b.** Results of *in situ*
567 hybridization (ISH) for DCHBV. (**a**) Positive signals are observed in both the nuclei
568 (arrows) and cytoplasm of normal hepatocytes. The cytoplasmic signals appear as
569 fine granules. ISH. (**b**) Positive signals are observed in both the nuclei (arrows) and
570 cytoplasm of neoplastic cells. The cytoplasmic signals appear as fine granules. ISH.

571 **References**

572 1. Adıgüzel E, Erdem-Şahinkesen E, Koç BT, Demirden C, Oğuzoğlu TÇ. The
573 detection and full genomic characterization of domestic cat Orthohepadnaviruses
574 from Türkiye. *Vet Med Sci*. 2023;9(5):1965–1972.
575 2. Aghazadeh M, Shi M, Barrs VR, *et al.* A Novel Hepadnavirus Identified in an
576 Immunocompromised Domestic Cat in Australia. *Viruses*. 2018;10(5):269.
577 3. Anderson LJ, Sandison AT. Tumors of the liver in cattle, sheep and pigs. *Cancer*.
578 1968;21(2):289–301.
579 4. Andrade RLFS, Dantas AFM, Pimentel LA, *et al.* Platynosomum fastosum-induced
580 cholangiocarcinomas in cats. *Vet Parasitol*. 2012;190(1–2):277–280.
581 5. Anpuanandam K, Selvarajah GT, Choy MMK, *et al.* Molecular detection and
582 characterisation of Domestic Cat Hepadnavirus (DCH) from blood and liver
583 tissues of cats in Malaysia. *BMC veterinary research*.2021;17(1):9.
584 6. Barrantes Murillo DF, Cattley RC, Cullen JM, *et al.* Intrahepatic mucinous
585 cholangiocarcinoma with recurrent colic in a horse case report and literature
586 review of cholangiocarcinoma in horses. *J Vet Diagn Invest*. 2024;36(4):547–
587 553.y
588 7. Bartenschlager R, Junker-Niepmann M, Schaller H. The P gene product of
589 hepatitis B virus is required as a structural component for genomic RNA
590 encapsidation. *J Virol*. 1990;64(11):5324–5332.
591 8. Bartenschlager R, Schaller H. The amino-terminal domain of the hepadnaviral P-
592 gene encodes the terminal protein (genome-linked protein) believed to prime
593 reverse transcription. *EMBO j*. 1998;7(13):4185–4192.

9. Bastianello SS. A survey on neoplasia in domestic species over a 40-year period from 1935 to 1974 in the Republic of South Africa. I. Tumours occurring in cattle. *Onderstepoort J Vet Res*. 1982;49(4):195–204.
10. Bastianello SS. A survey of neoplasia in domestic species over a 40-year period from 1935 to 1974 in the Republic of South Africa. V. Tumours occurring in the cat. *Onderstepoort J Vet Res*. 1983;50(2):105–110.
11. Bastianello SS. A survey on neoplasia in domestic species over a 40-year period from 1935 to 1974 in the Republic of South Africa. VI. Tumours occurring in dogs. *Onderstepoort J Vet Res*. 1983;50(3):199–220.
12. Beasley RP, Hwang LY, Lin CC, *et al.* Hepatocellular carcinoma and hepatitis B virus. A prospective study of 22 707 men in Taiwan. *Lancet*. 1981;2(8256):1129–1133.
13. Berto AN, Lemos GAA, Navolar FMN, Di Santis GW, Zanutto MS. Metastatic pancreatic carcinoma with neuroendocrine differentiation in a cat. JFMS Open Rep. 2024;10(1):20551169231213504.
14. Bettini G, Marcato PS. Primary hepatic tumours in cattle. A classification of 66 cases. *J Comp Pathol*. 1992;107(1):19–34.
15. Brechot C, Pourcel C, Louise A, *et al.* Presence of integrated hepatitis B virus DNA sequences in cellular DNA of human hepatocellular carcinoma. *Nature*. 1980;286(5772):533–535.
16. Brindley PJ, Melinda Bachini, Sumera I. Ilyas, *et al.* Cholangiocarcinoma. *Nat Rev Dis Primers*. 2021;7(1):65.
17. Capozza P, Maura Carrai, Yan Ru Choi, *et al.* Domestic Cat Hepadnavirus: Molecular Epidemiology and Phylogeny in Cats in Hong Kong. *Viruses*. 2023;15(1):150.

18. Carpenter JL, Andrews IK. Tumors and tumor-like lesions. In: Holzworth J, ed. Diseases of the Cat. Saunders; 1987:406–AD.
19. Chang HP. HEPATIC CLONORCHIASIS AND CARCINOMA OF THE BILE DUCT IN A DOG. *J Pathol Bacteriol*. 1965;89:365–367.
20. Chang HP. PATHOLOGICAL CHANGES IN THE INTRAHEPATIC BILE DUCTS OF CATS (FELIS CATUS) INFESTED WITH CLONORCHIS SINENSIS. *J Pathol Bacteriol*. 1965;89:357–364.
21. Conti MB, Marchesi MC, Zappulla F, *et al.* Clinical findings and diagnosis in a case of cholangiocellular carcinoma in a horse. *Vet Res Commun*. 2008;32(Suppl 1):S271-273.
22. Cullen JM. Tumors of the liver and gallbladder. In: Meuten DJ, ed. *Tumors in Domestic Animals*. 5th ed. John Wiley & Sons; 2017:617–621.
23. Diakoudi G, Capozza P, Lanave G, *et al.* A novel hepadnavirus in domestic dogs. *Sci Rep*. 2022;12(1):2864.
24. Domínguez MC, Chávez G, Trigo FJ, Rosales ML. Concurrent cholangiocarcinoma, peritonitis, paratuberculosis, and aspergillosis in a goat. *Can Vet J*. 2001;42(11):884–885.
25. Fujimoto A, Furuta M, Totoki Y, *et al.* Whole-genome mutational landscape and characterization of noncoding and structural mutations in liver cancer. *Nat Genet*. 2016;48(5):500–509.
26. Hayashi Y, Tajiri K, Ozawa T, *et al.* Impact of preS1 Evaluation in the Management of Chronic Hepatitis B Virus Infection. *Medicina (Kaunas)*. 2024;60(8):1334.
27. Hayes HM, Morin MM, Rubenstein DA. Canine biliary carcinoma: epidemiological comparisons with man. *J Comp Pathol*. 1983;93(1):99–107.

643 28. Head KW, Else RW, Dubielzig RR. Tumors of the liver. In: Head KW, Else RW,
644 Dubielzig RR, eds. *Histological Classification of Tumors of the Alimentary System*
645 *of Domestic Animals*. 2nd ed. Armed Forces Institute of Pathology; 2003:121–
646 126.
647 29. Hirao K, Matsumura K, Imagawa A, Enomoto Y, Hosogi Y. Primary neoplasms in
648 dog liver induced by diethylnitrosamine. *Cancer Res*. 1974;34(8):1870–1882.
649 30. Hirose N, Uchida K, Kanemoto H, Ohno K, Chambers JK, Nakayama H. A
650 retrospective histopathological survey on canine and feline liver diseases at the
651 University of Tokyo between 2006 and 2012. *Journal Vet Med Sci*.
652 2014;76(7):1015–1020.
653 31. Hou PC. PRIMARY CARCINOMA OF BILE DUCT OF THE LIVER OF THE CAT
654 (FELIS CATUS) INFESTED WITH CLONORCHIS SINENSIS. *J Pathol Bacteriol*,
655 1964;87:239–244.
656 32. Hu J, Flores D, Toft D, Wang X, Nguyen D. Requirement of heat shock protein 90
657 for human hepatitis B virus reverse transcriptase function. *J Virol*.
658 2004;78(23):13122–13131.
659 33. Imazeki F, Yaginuma K, Omata M, Okuda K, Kobayashi M, Koike K. Integrated
660 structures of duck hepatitis B virus DNA in hepatocellular carcinoma. *J Virol*.
661 1988;62(3):861–865.
662 34. Jakab Cs, Kiss A, Schaff Zs, *et al.* Claudin-7 protein differentiates canine
663 cholangiocarcinoma from hepatocellular carcinoma. *Histol Histopathol*.
664 2010;25(7):857–864.
665 35. Jeanes EC, Wegg ML, Mitchell JA, Priestnall SL, Fleming L, Dawson C.
666 Comparison of the prevalence of Domestic Cat Hepadnavirus in a population of

667 cats with uveitis and in a healthy blood donor cat population in the United
668 Kingdom. *Vet Ophthalmol*. 2022;25(2):165–172.
669 36. Jones SA, Clark DN, Cao F, Tavis JE, Hu J. Comparative analysis of hepatitis B
670 virus polymerase sequences required for viral RNA binding, RNA packaging, and
671 protein priming. *J Virol*. 2014;88(3):1564–1572.
672 37. Kim S, Lee J, Ryu W-S. Four conserved cysteine residues of the hepatitis B virus
673 polymerase are critical for RNA pregenome encapsidation. *J Virol*,
674 2009;83(16):8032–8040.
675 38. Kim Y, Hong YB, Jung G. Hepatitis B virus: DNA polymerase activity of deletion
676 mutants. *Biochem Mol Biol Int*, 1999;47(2):301–308.
677 39. Lanave G, Capozza P, Diakoudi G, *et al.* Identification of hepadnavirus in the sera
678 of cats. *Sci Rep*. 2019;9(1): 10668.
679 40. Lanford RE, Chavez D, Brasky KM, R B Burns 3rd, R Rico-Hesse. Isolation of a
680 hepadnavirus from the woolly monkey, a New World primate. *Proc Natl Acad Sci*
681 *U S A*. 1998;95(10):5757–5761.
682 41. Lanford RE, Kim YH, Lee H, Notvall L, Beames B. Mapping of the hepatitis B
683 virus reverse transcriptase TP and RT domains by transcomplementation for
684 nucleotide priming and by protein-protein interaction. *J Virol*, 1999;73(3):1885–
685 1893.
686 42. Lawrence HJ, Erb HN, Harvey HJ. Nonlymphomatous hepatobiliary masses in
687 cats: 41 cases (1972 to 1991). *Vet Surg*. 1994;23(5):365–368.
688 43. Lin B, He Q, Lu Y, Zhang W, Jin J, Pan H. Viral hepatitis increases the risk of
689 cholangiocarcinoma: a systematic review and meta-analysis. *Transl Cancer Res*.
690 2023;12(6):1602–1616.

44. Lourenço J, McNaughton AL, Pley C, Obolski U, Gupta S, Matthews PC. Polymorphisms predicting phylogeny in hepatitis B virus. *Virus Evol*. 2022;9(1):veac116.
45. MacVean DW, Monlux AW, Anderson PS Jr, Silberg SL, Roszel JF. Frequency of canine and feline tumors in a defined population. *Vet Pathol*. 1978;15(6):700–715.
46. Madsen T, Arnal A, Vittecoq M, *et al*. Cancer prevalence and etiology in wild and captive animals. In: Aktipis CA, Maley CC, eds. *Ecology and Evolution of Cancer*. Academic Press; 2017:11–46.
47. Magnius L, Mason WS, Taylor J, *et al.* ICTV Virus Taxonomy Profile: Hepadnaviridae. *J Gen Virol*. 2020;101(6):571–572.
48. Maronpot RR, Giles HD, Dykes DJ, Irwin RD. Furan-induced hepatic cholangiocarcinomas in Fischer 344 rats. *Toxicol Pathol*. 1991;19(4 Pt 2):561–570.
49. Niwa H, Yamamura K, Miyazaki J. Efficient selection for high-expression transfectants with a novel eukaryotic vector. *Gene*. 1991;108(2):193–199.
50. Nomoto K, Tsuneyama K, Cheng C, *et al.* Intrahepatic cholangiocarcinoma arising in cirrhotic liver frequently expressed p63-positive basal/stem-cell phenotype. *Pathol Res Pract*. 2006;202(2):71–76.
51. Pandolfo GW, Teixeira MBS, de Cristo TG, Gaspar T, Carniel F, Casagrande RA. Metastatic gallbladder adenocarcinoma in a cat. *Brazilian Journal of Veterinary Pathology*, 2023;16(2):117–121.
52. Patnaik AK, Liu SK, Hurvitz AI, McClelland AJ. Nonhematopoietic neoplasms in cats. *J Natl Cancer Inst*. 1975;54(4):855–860.
53. Patnaik AK, Hurvitz AI, Lieberman PH, Johnson GF. Canine bile duct carcinoma. *Vet Pathol*. 1981;18(4):439–444.

716 54. Patnaik, A.K. A morphologic and immunocytochemical study of hepatic neoplasms
717 in cats. *Vet Pathol*. 1992;29(5):405–415.
718 55. Pesavento PA, Jackson K, Hampson TSTTB, Munday JS, Barrs VR, Beatty JA. A
719 Novel Hepadnavirus is Associated with Chronic Hepatitis and Hepatocellular
720 Carcinoma in Cats. *Viruses*. 2019;11(10):969.
721 56. Piewbang C, Wardhani SW, Chaiyasak S, *et al*. Insights into the genetic diversity,
722 recombination, and systemic infections with evidence of intracellular maturation of
723 hepadnavirus in cats. *PloS One*. 2020;15(10):e0241212.
724 57. Pley C, Lourenço J, McNaughton AL, Matthews PC. Spacer Domain in Hepatitis B
725 Virus Polymerase: Plugging a Hole or Performing a Role?. *J Virol*.
726 2022;96(9):e0005122.
727 58. Radziwill G, Tucker W, Schaller H. Mutational analysis of the hepatitis B virus P
728 gene product: domain structure and RNase H activity. *J Virol*. 1990;64(2):613–
729 620.
730 59. Ramos JA, Vara, Borst LB. Immunohistochemistry: fundamentals and applications
731 in oncology. In: Meuten DJ, ed. *Tumors in Domestic Animals*. 5th ed. John Wiley
732 & Sons; 2017:44–87.
733 60. Roy S, Glaser S, Chakraborty S. Inflammation and Progression of
734 Cholangiocarcinoma: Role of Angiogenic and Lymphangiogenic Mechanisms.
735 *Front Med (Lausanne)*. 2019;6:293.
736 61. Shofa M, Ohkawa A, Okabayashi T, Kaneko Y, Saito A. Development of a direct
737 duplex real-time PCR assay for rapid detection of domestic cat hepadnavirus. *J
738 Vet Diagn Invest Official Publication of the American Association of Veterinary
739 Laboratory Diagn Invest*. 2023;35(2):139–144.

62. Silva BB, Chen JY, Villanueva BH, *et al.* Genetic Diversity of Domestic Cat Hepadnavirus in Southern Taiwan. *Viruses*. 2023;15(10):2128.
63. Sivanand A, Talati D, Kalariya Y, Patel P, Gandhi SK. Associations of Liver Fluke Infection and Cholangiocarcinoma: A Scoping Review. *Cureus*. 2023;15(10):e46400.
64. Song Z, Lin S, Wu X, *et al.* Hepatitis B virus-related intrahepatic cholangiocarcinoma originates from hepatocytes. *Hepatol Int*. 2023;17(5):1300–1317.
65. Sripa B, Kaewkes S, Sithithaworn P, *et al.* Liver fluke induces cholangiocarcinoma. *PLoS Med*. 2007;4(7):e201.
66. Sternberg SS, Popper H, Oser BL, Oser M. Gallbladder and bile duct adenocarcinomas in dogs after long term feeding of aramite. *Cancer*. 1960;13:780–789.
67. Stone C, Petch R, Gagne RB, *et al.* Prevalence and Genomic Sequence Analysis of Domestic Cat Hepadnavirus in the United States. *Viruses*. 2022;14(10):2091.
68. Strafuss AC. Bile duct carcinoma in dogs. *J Am Vet Med Assoc*. 1976;169(4):429.
69. Summers J, Smolec JM, Snyder R. A virus similar to human hepatitis B virus associated with hepatitis and hepatoma in woodchucks. *Proc Natl Acad Sci U S A*. 1978;75(9):4533–4537.
70. Takahashi K, Kaneko Y, Shibanai A, *et al.* Identification of domestic cat hepadnavirus from a cat blood sample in Japan. *J Vet Med Sci*. 2022;84(5):648–652.
71. Taylor GN, Lloyd RD, Mays CW, *et al*. Plutonium- or americium-induced liver tumors and lesions in beagles. *Health Phys*. 1991;61(3):337–347.

764 72. Tessmann A, Sumienski J, Sita A, *et al.* Domestic cat hepadnavirus genotype B is
765 present in Southern Brazil. *Virus Genes*. 2025;61(1):81–86.
766 73. Trigo FJ, Thompson H, Breeze RG, Nash AS, *et al*. The pathology of liver
767 tumours in the dog. *J Comp Pathol*. 1982;92(1):21–39.
768 74. Tsuchiya J, Miyoshi M, Kakinuma S, *et al*. Hepatitis B Virus-KMT2B Integration
769 Drives Hepatic Oncogenic Processes in a Human Gene-edited Induced
770 Pluripotent Stem Cells-derived Model. *Cell Mol Gastroenterol Hepatol*.
771 2025;19(2):101422.
772 75. Wang C, Wang MD, Cheng P, *et al*. Hepatitis B virus X protein promotes the stem-
773 like properties of OV6+ cancer cells in hepatocellular carcinoma. *Cell Death Dis*.
774 2017;8(1): e2560.
775 76. Whitehead JE. Neoplasia in the cat. *Vet Med Small Anim Clin*. 1967;62(1):44–45.
776

Figure 1

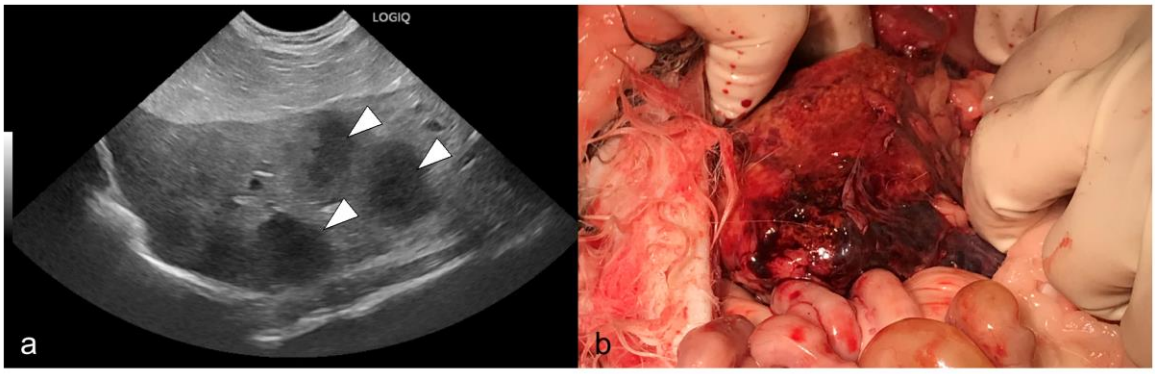

Figure 2

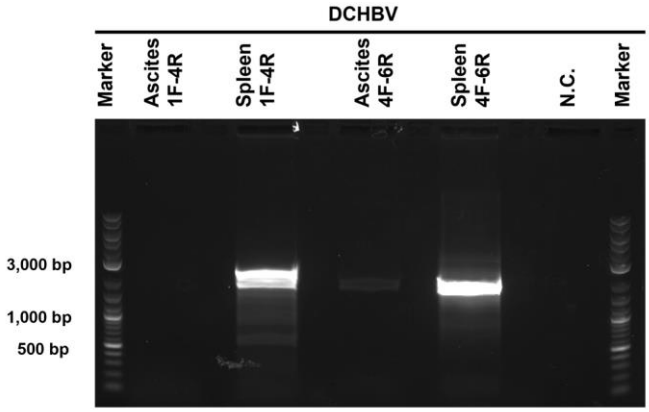

Figure 3

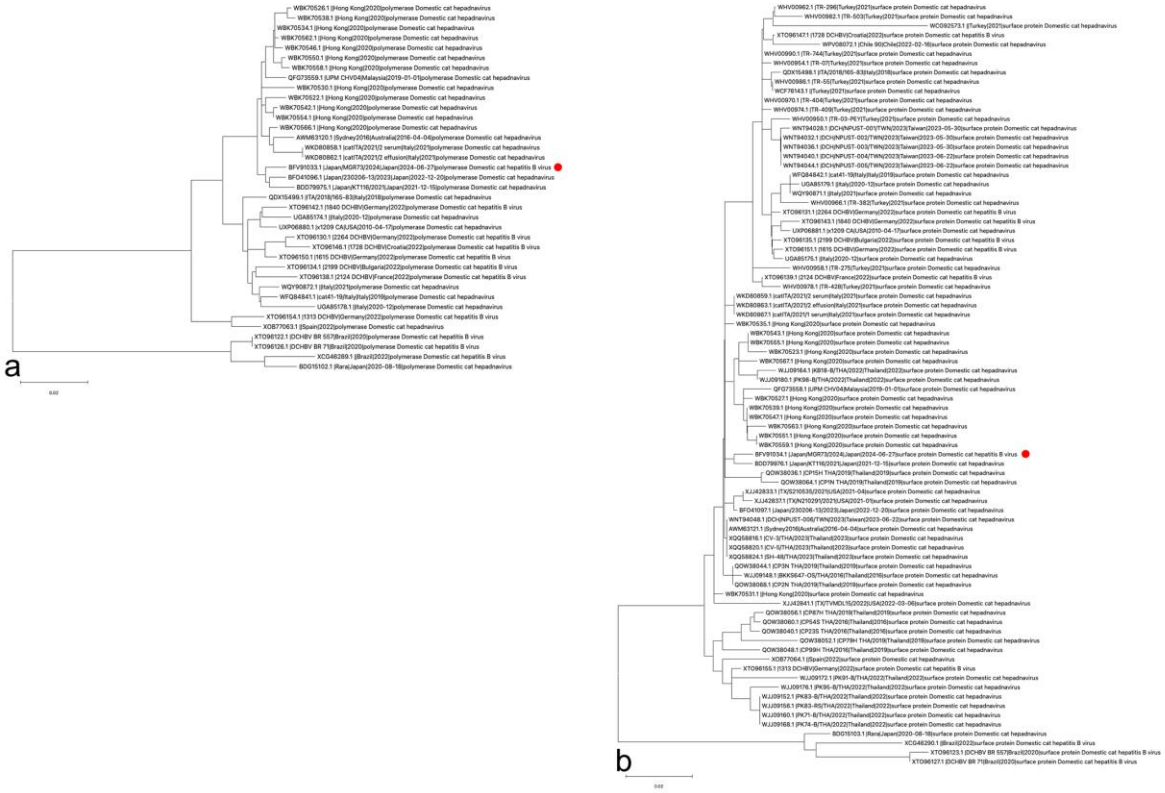

779

Figure 3

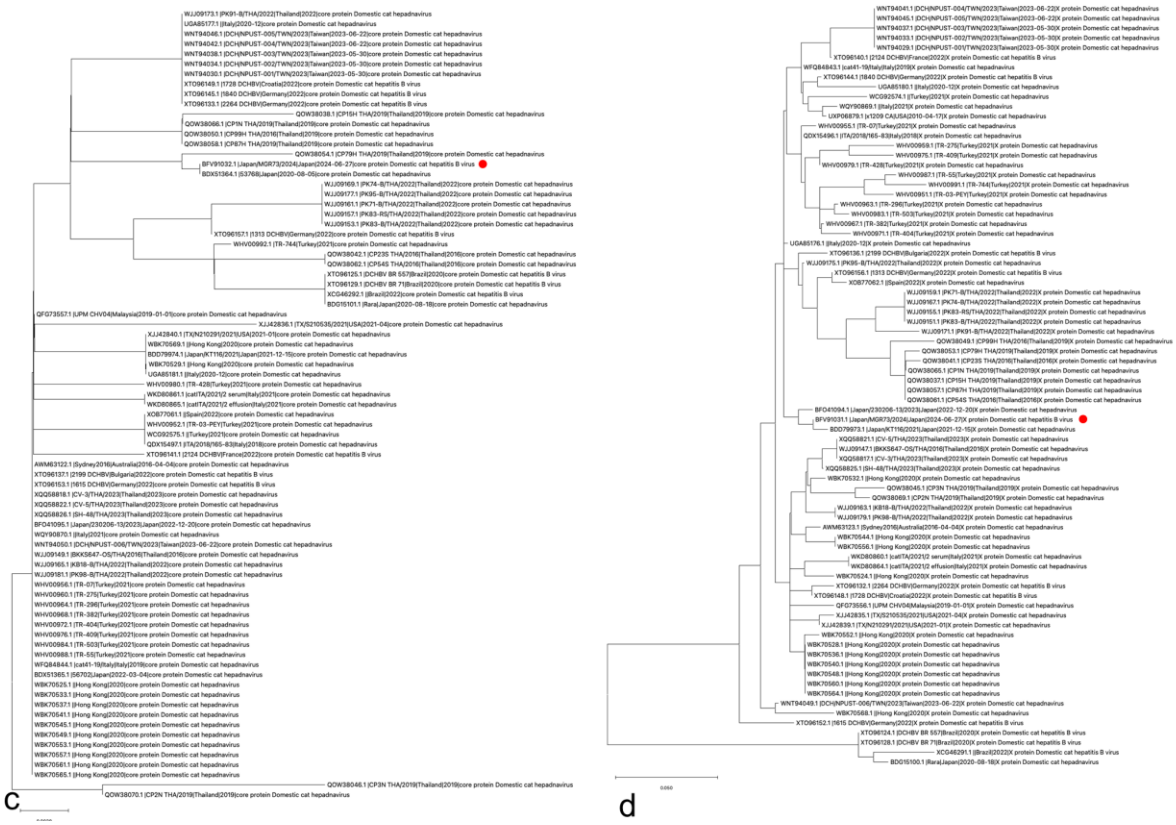

780

Figure 3

Figure 3

f

Species/Abbrv	*	*	*																		*	*	*
1. Sydney2016	C	C	A	A	T	C	A	C	C	A	A	T	C	C	T	C	C	T	C	C	T		
2. Japan/KT116/2021	C	C	A	A	T	C	A	C	C	A	A	T	C	C	T	-	-	-	C	C	T		
3. JAPAN/MGR73/2024-Spleen	C	C	A	-	-	-	-	-	-	-	-	-	-	-	-	-	-	-	C	C	T		
4. JAPAN/MGR73/2024-Liver	C	C	A	-	-	-	-	-	-	-	-	-	-	-	-	-	-	-	C	C	T		

Figure 4

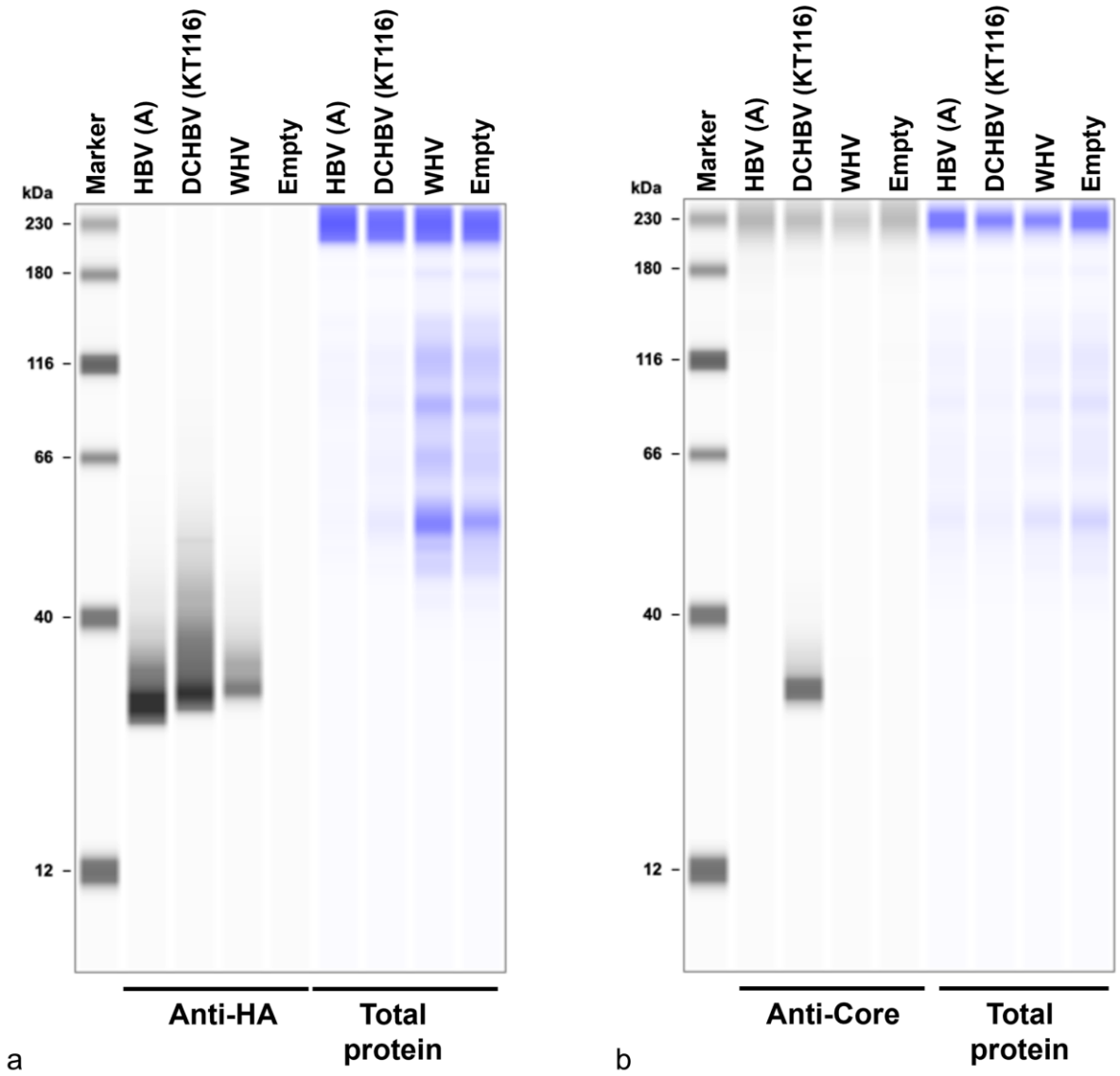
Marker
HBV (A)
DCHBV (KT116)
WHV
Empty
HBV (A)
DCHBV (KT116)
WHV
Empty
kDa
230
180
116
66
40
12
Anti-HA
Total protein
a
Marker
HBV (A)
DCHBV (KT116)
WHV
Empty
HBV (A)
DCHBV (KT116)
WHV
Empty
kDa
230
180
116
66
40
12
Anti-Core
Total protein
b

783

Figure 5

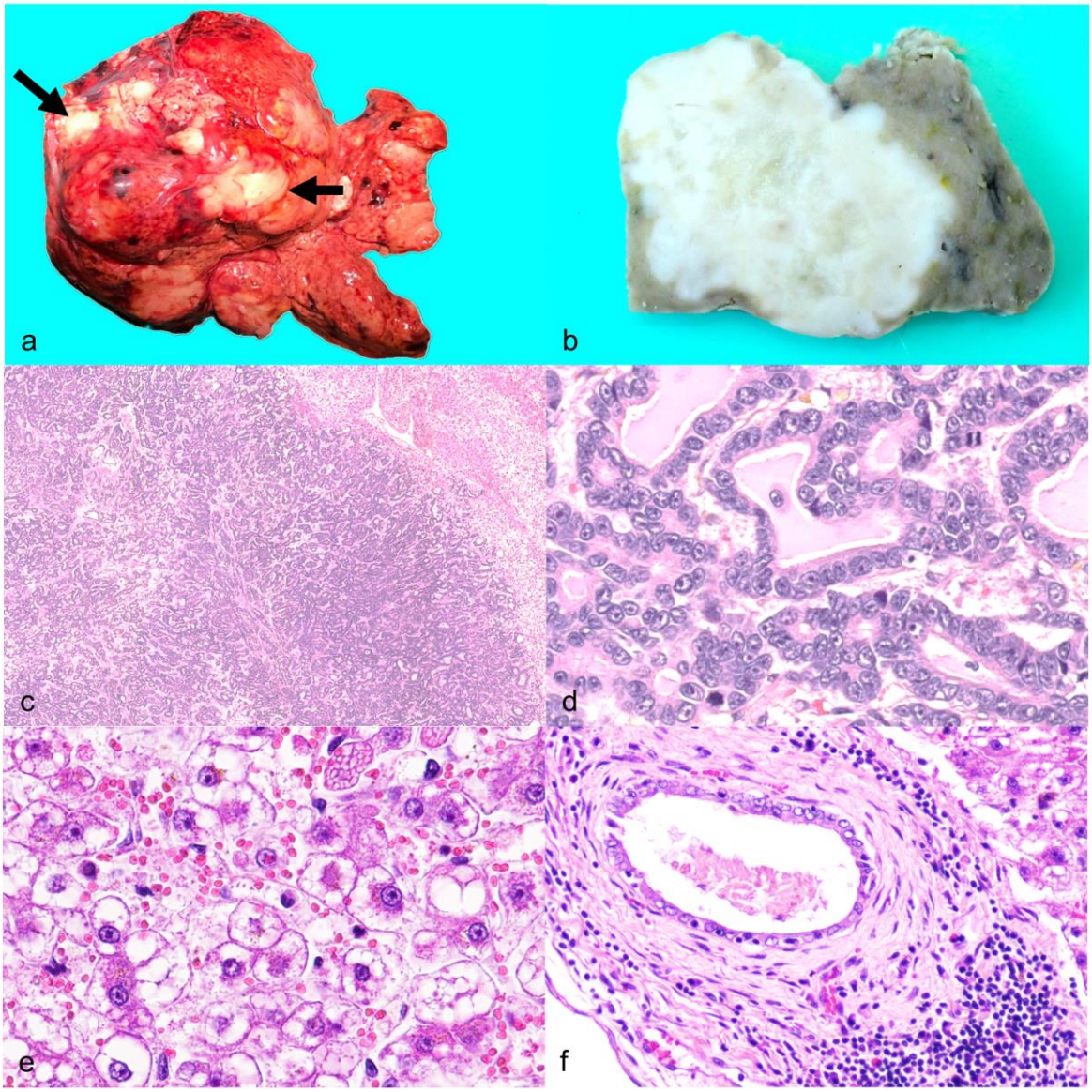

784

Figure 6

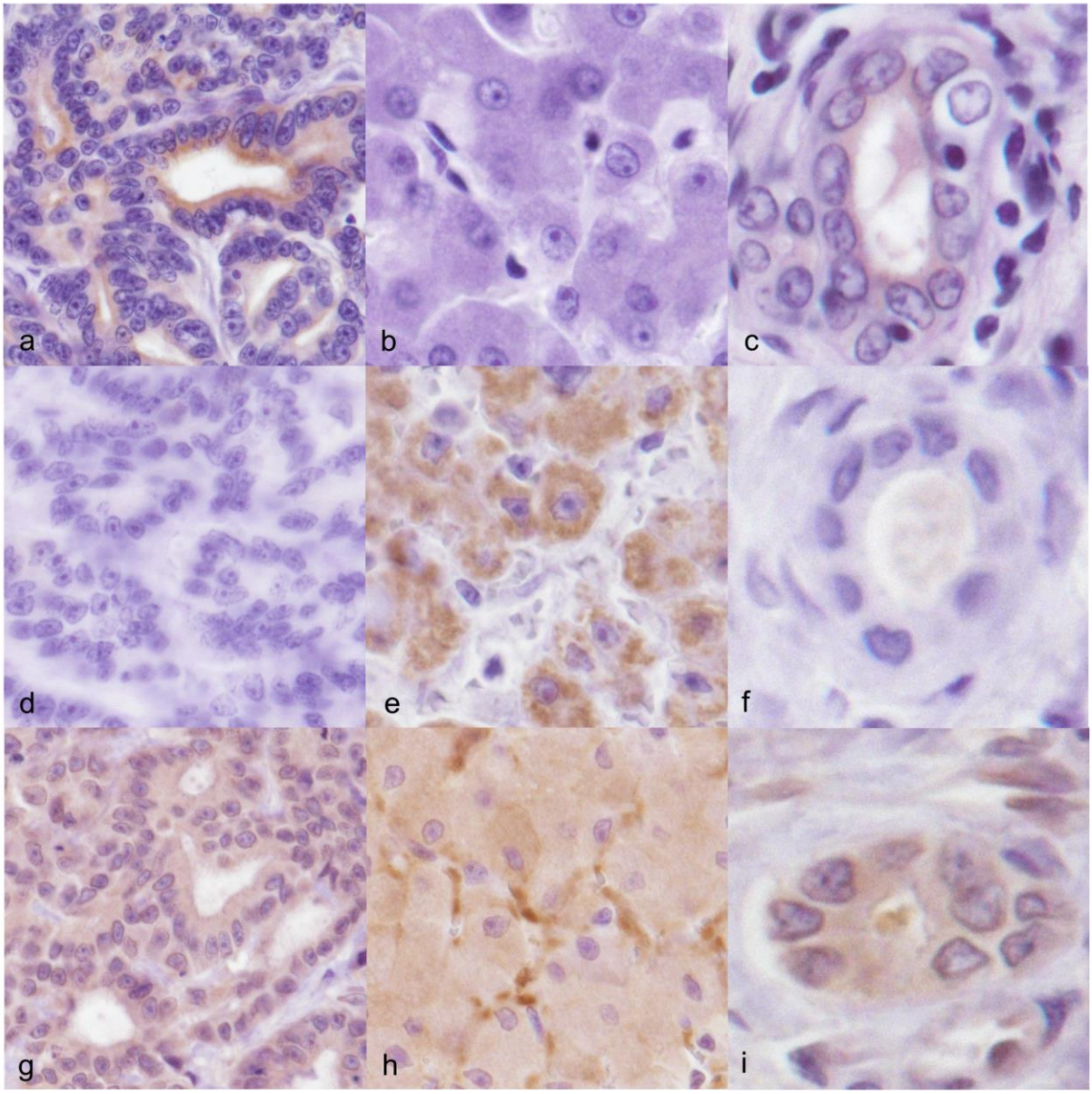

785

Figure 7

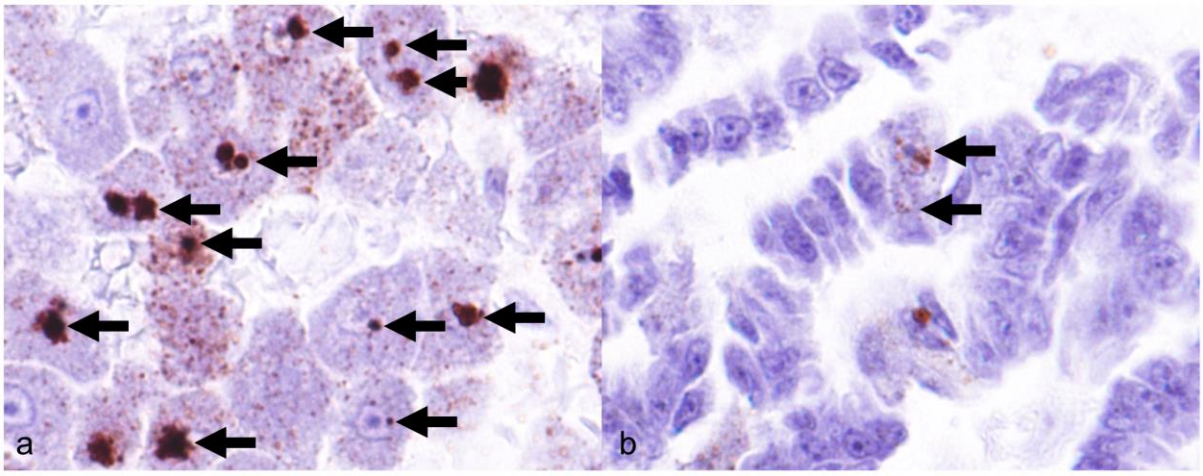

786